

The Search for Exotic Mesons in $\eta\pi^-$ from Photoproduction with CLAS

Diane Schott^{*†}

The George Washington University

E-mail: dschott@jlab.org

Over twenty years ago QCD-inspired models of hadronic states suggested the existence of mesons beyond the Naive Quark Model (NQM), which motivated a rigorous search for exotic mesons. The lightest of these states is the $\pi_1(1400)$ decaying to $\eta\pi^-$ observed by experiment E852 at Brookhaven [1] and the VES collaboration at IHEP. Photoproduction is predicted to favor production of a $J^{PC} = 1^{-+}$ gluonic excitation resulting in the increase of the ratio of π_1 to a_2 mesons. A Partial Wave Analysis was conducted on the reaction $\gamma p \rightarrow \Delta^{++} X \rightarrow p\pi^+\pi^-(\eta)$, using the Δ^{++} to select the pion exchange. The analysis has shown the final spectra of the resonance decaying to $\eta\pi^-$ to be dominated by the quantum state of $J^{PC} = 2^{++}$ corresponding to the presence of the $a_2(1320)$. The $J^{PC} = 1^{-+}$ state, shows no structure in the intensity distribution. The phase difference between the $J^{PC} = 1^{-+}$ and $J^{PC} = 2^{++}$ amplitudes show the interference between the two states. The PWA mass independent fits, along with the mass dependent fits of the partial wave results, will be shown for the $\eta\pi^-$.

Xth Quark Confinement and the Hadron Spectrum

8-12 October 2012

TUM Campus Garching, Munich, Germany

^{*}Speaker.

[†]All of this wouldn't be possible without the support from the g12 experiment group and the CLAS collaboration.

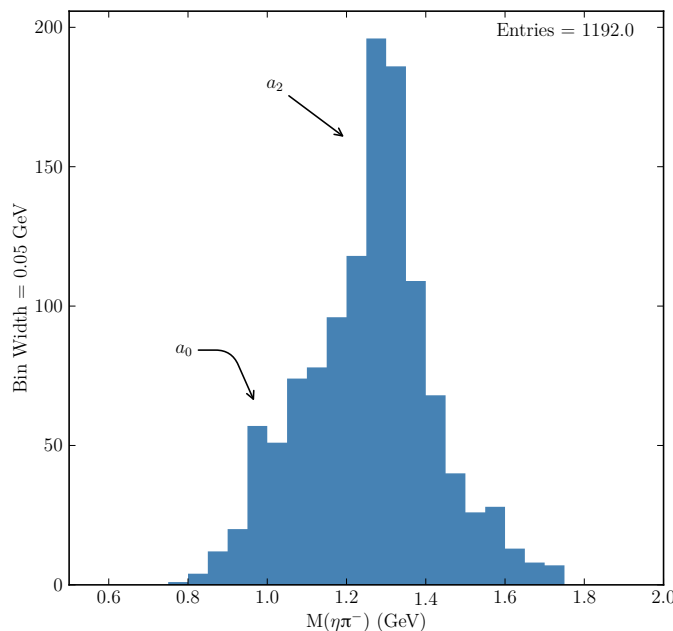


Figure 1: Invariant mass of $\eta\pi^-$ binned for the PWA fit. The arrows point out the mass range of where the a_0 and a_2 resonances would be expected.

1. Introduction

Despite having explored exotic mesons using hadron beams, there is very limited data on photoproduction of light-quark mesons. It has been predicted that exotic mesons will be produced with intensities 10 times that seen using hadron beams [2]. Of the light meson photoproduction experiments that have been done, the statistics have been low, making a partial wave analysis (PWA) difficult and inconclusive [3, 4].

2. Data Selection

The data were taken at Jefferson Lab in Newport News, VA to study light mesons in the 1 to 2 GeV mass range from γp interactions with $E_\gamma = 4.4$ to 5.6 GeV. This experiment was run in Hall B using the CLAS spectrometer. The reconstruction of the η was calculated from the missing four-momentum from the reconstructed charged tracks. To select the Δ^{++} , a cut on the $p\pi^+$ invariant mass selecting events with a mass less than 1.3 GeV. An additional cut on the momentum transfer, t , was employed to select the forward going $\eta\pi^-$ from the slower moving baryon background. The final events to be fit are shown in Fig. 1. To separate these states, partial wave analysis was employed.

3. Formalism

The formalism used in this analysis is based on Chung [5, 6, 7], as used in the E852 [1, 8, 9]

and g6c [10] analysis. The intensity of the resonance X is:

$$I = \left| \sum_{\alpha} V_{\alpha} A_{\alpha} \right|^2 \quad (3.1)$$

where the V is unknown production amplitude and A is the decay amplitude derived from the measured distributions of the kinematic variables of the η and π^- . The sum is over all quantum numbers that describe X , where α is the set $\{J, P, M, L, I, \lambda, S\}$.

To find the decay amplitudes, A , the state of the resonance X is described by J , M , L , and S . X decays to η and π^- where they are described by the kinematic variables in the rest frame of X . Where p is the momentum of η with a direction given by θ_{η} and ϕ_{η} , these are known as the Gottfried-Jackson angles. The decay amplitude is

$$A_{J,M,L,S}(\theta_{\eta}, \phi_{\eta}) = \sum_{\lambda} \tilde{L} \tilde{S} D_{M\lambda}^{J*}(\theta_{\eta}, \phi_{\eta}, 0) (LOS\lambda | S\lambda) (S_{\eta} \lambda_{\eta} S_{\pi^-} - \lambda_{\pi^-} | S\lambda) F_L(p) a_{LS} \quad (3.2)$$

where $F_L(p)$ is the barrier function, which in this analysis is the Blatt-Weisskopf centrifugal-barrier function for correcting the amplitude near threshold [11]. The detailed derivation of the intermediate steps is explained in detailed in Ref. [12] for the decay to two-particle states.

The amplitudes are constructed as eigenstates of reflectivity to take advantage of the parity conservation in the production process [13]. It reduces the possible number of external spin configurations by a factor of two. Essentially, the sign of the quantum number M becomes the reflectivity, ε , and M is now the absolute value of the initial M . Breaking the amplitudes into eigenstates of ε results in the intensity distribution for a photon beam of:

$$I(\theta_{\eta}, \phi_{\eta}) = \sum_{\varepsilon} \rho_{\varepsilon\varepsilon'} \left| \sum_{\alpha} {}^{\varepsilon}V_{\alpha}(\theta_{\eta}, \phi_{\eta}) {}^{\varepsilon}A_{\alpha}(\theta_{\eta}, \phi_{\eta}) \right|^2, \quad (3.3)$$

where ${}^{\varepsilon}V_{\alpha}(\theta_{\eta}, \phi_{\eta})$ and ${}^{\varepsilon}A_{\alpha}(\theta_{\eta}, \phi_{\eta})$ are the production and decay amplitudes for a given reflectivity, ε .

The photon spin-density matrix in the reflectivity basis for unpolarized and circularly polarized photon beam is $\frac{1}{2}$ times the identity matrix. In the case of a circularly polarized beam, states with different reflectivities cannot interfere with each other but waves of the same reflectivity can. The decay amplitude rewritten to include reflectivity is defined as

$${}^{\varepsilon}A_{\alpha}(\theta_{\eta}, \phi_{\eta}) = \Theta(M) (A_{\alpha}^M(\theta_{\eta}, \phi_{\eta}) - \varepsilon P(-1)^{J-M} A_{\alpha}^{-M}(\theta_{\eta}, \phi_{\eta})) \quad (3.4)$$

where $\Theta(M)$ is $\frac{1}{\sqrt{2}}$ or $\frac{1}{2}$ for $M > 0$ and $M = 0$, respectively [5].

The likelihood, L , is the product of the probability for each event in the bin. For the partial wave analysis, the probability is the intensity distribution over the variables θ_{η} and ϕ_{η} . The likelihood is defined as:

$$L = \exp(-\bar{N}_o({}^{\varepsilon}V_{\alpha})) \prod_i^{N_o} I(\theta_{\eta i}, \phi_{\eta i}), \quad (3.5)$$

where $I(\theta_{\eta i}, \phi_{\eta i})$ is the intensity distribution for an individual bin in the angles ϕ_{η} and θ_{η} from equation 3.3 [3]. $\bar{N}_o({}^{\varepsilon}V_{\alpha})$ is the average number of events observed if the exact experiment was repeated several times for a given ${}^{\varepsilon}V_{\alpha}$. $\bar{N}_o({}^{\varepsilon}V_{\alpha})$ takes into account the acceptance of the experiment and is evaluated using Monte Carlo simulations to model the reaction in the detector configuration.

Since the likelihood function is a product of probabilities over the number of events in a given $\eta\pi^-$ mass bin, it becomes large very quickly. For practical reasons it is the $-\ln(L)$ that is minimized during the fitting procedure with the production amplitudes varied to find the minimum $-\ln(L)$. Expanding the likelihood function yields:

$$\ln L = \sum_i^{N_o} \ln \sum_{\varepsilon, \varepsilon', \alpha, \alpha'} \rho_{\varepsilon\varepsilon'} \varepsilon V_\alpha \varepsilon' V_{\alpha'}^* \varepsilon A_\alpha(\theta_{\eta i}, \phi_{\eta i}) \varepsilon' A_{\alpha'}^*(\theta_{\eta i}, \phi_{\eta i}) \quad (3.6)$$

$$- N_o \frac{N_r}{N_\eta} \sum_{\varepsilon, \varepsilon', \alpha, \alpha'} \varepsilon V_\alpha \varepsilon' V_{\alpha'}^* \varepsilon \varepsilon' \Phi_{\alpha\alpha'}^\eta, \quad (3.7)$$

where

$$\varepsilon \varepsilon' \Phi_{\alpha\alpha'}^\eta = \frac{1}{N_\eta} \sum_i^{N_\eta} \rho_{\varepsilon\varepsilon'} \varepsilon A_\alpha(\theta_{\eta i}, \phi_{\eta i}) \varepsilon A_{\alpha'}^*(\theta_{\eta i}, \phi_{\eta i}), \quad (3.8)$$

[3] and $\varepsilon \varepsilon' \Phi_{\alpha\alpha'}^\eta$ is the normalized acceptance integral calculated from the amplitudes of the accepted simulated data. From the simulation, N_r is the number of raw events and N_η is the number of events accepted. N_o is the number of observed events in the data. The $\varepsilon A_{\alpha'}^*(\theta_{\eta i}, \phi_{\eta i})$ are the amplitudes calculated for all data events.

4. Partial Wave Fitting Procedure

The fitting program is setup with the same structure as documented in [11]. The program is designed to call the MINUIT minimization package in the CERNLIB library and fits equation 3.7 to determine the real and imaginary parts of the production amplitude, $Re(\varepsilon V_\alpha)$ and $Im(\varepsilon V_\alpha)$, respectively, for each of the partial wave states. The acceptance corrected yield for an individual mass bin is defined by

$$N = N_o \frac{N_r}{N_\eta} \sum_{\varepsilon, \alpha, \alpha'} \varepsilon V_\alpha \varepsilon V_{\alpha'}^* \varepsilon \Phi_{\alpha\alpha'}^\eta \quad (4.1)$$

where $\varepsilon \Phi_{\alpha\alpha'}^\eta$ is raw normalization integral calculated from the amplitudes of the raw generated events.

The acceptance corrected yields plotted as a function of resonance mass are used to extract a mass and width of the peak in a partial wave state. This process is referred to as a mass-dependent fit. The phase difference between two wave states is

$$\Delta\Phi = \arctan\left(\frac{Im(\varepsilon V_\alpha \varepsilon V_{\alpha'}^*)}{Re(\varepsilon V_\alpha \varepsilon V_{\alpha'}^*)}\right). \quad (4.2)$$

The phase difference between the complex variables, $\varepsilon V_{k\alpha}$ and $\varepsilon V_{k\alpha'}^*$, can show interference between wave states and can be fitted for the masses and widths of these states.

5. Partial Wave Analysis

5.1 Wave Set

For the meson mass range of 1.0 to 1.6 GeV, the higher order states are not expected so the included states are $J < 3$. Additionally, the photon has a spin of ± 1 further constraining the spin

projection of the resonance to be $m\mathcal{E} = 1\pm$. The final wave set is P_1 , D_1 , and S_0 . The S_0 is included to absorb the background that is not described by the other partial waves. The S wave has an isotropic intensity, in θ and ϕ , where the P and D waves are not. With the circularly polarized photon beam, the positive and negative reflectivity states have equal contribution so the positive and negative reflectivity states are tied together in the fitter.

5.2 PWA: Mass-Independent Fit

The PWA was performed on a bin-by-bin basis of the $\eta\pi^-$ invariant mass with the fit parameters of each bin independent of the previous bin. For a given set of waves in each fit, ten fits were performed using random initial parameters and the final solution was chosen to be the result with the highest maximum likelihood value. Reiterating the fit avoids selecting a fit that could have found a local maximum, missing the best solution. The mass-independent fits have shown a large contribution from the $J^P|m| = 2^+1$ state, with defined peaks around the mass of the $a_2(1320)$ as expected from the quark model. The results of the final fit are included in the mass dependent fit results in Figs. 3, 4, and 5.

5.2.1 Fit Quality

To check the quality of the PWA fit, the solution is used to weight generated events, taking wave angle distributions and detector acceptance into account. In Fig. 2 the GJ angles are compared between the data and the prediction from the PWA solution. The conclusion of the mass-independent fit is the PWA solution describes the data very well for the GJ angles.

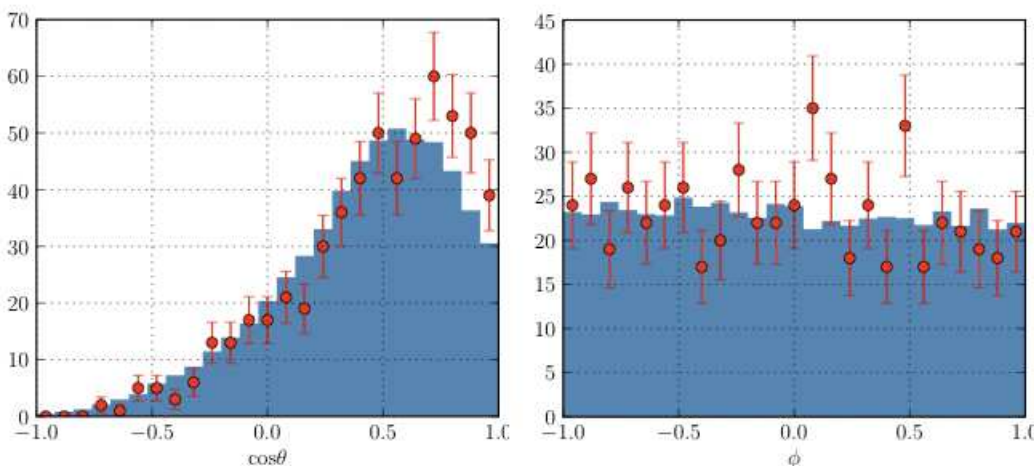


Figure 2: The GJ angles for the data (points) used in the PWA fit overlaid with the predicted distribution from the PWA solution (histogram).

5.3 Mass-Dependent Fit

To understand the nature of the P and D waves observed in this experiment, a mass-dependent fit is applied to the results of the PWA intensity and phase difference distributions. This fit was carried out over the $\eta\pi^-$ mass range of 1.0 to 1.7 GeV. The P and D wave decay amplitudes are

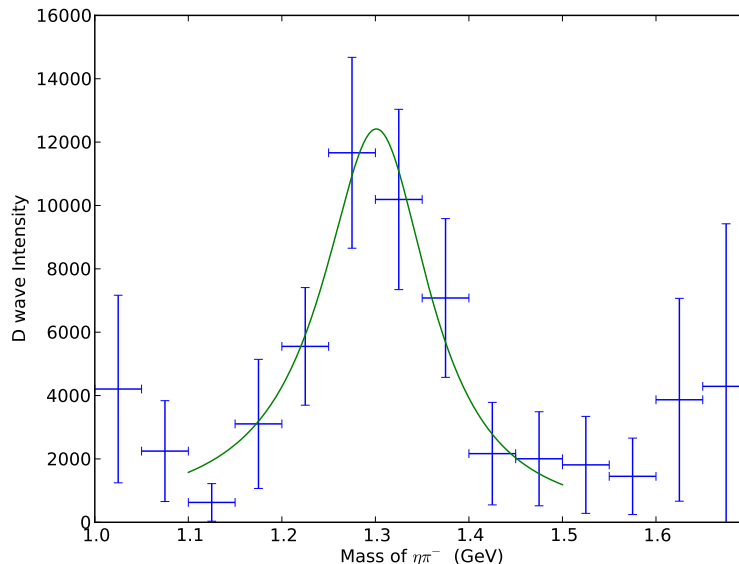


Figure 3: Fit 1: Intensity mass dependent fit for a_2 . Fitting the BW intensity function (Eq. ??), the mass and width of the a_2 is 1.32 ± 0.01 and 0.154 ± 0.011 GeV, includes both reflectivities added together.

treated as resonant and use the relativistic Breit-Wigner forms for the amplitudes. The fit of the intensity of the 2^{+1} for the a_2 is illustrated in Fig. 3 with a final mass and width of 1.32 ± 0.01 and 0.154 ± 0.011 GeV, respectively. The fit was used as the initial mass and width for the rest of the fits. The accepted mass and width of the a_2 is 1.318 and 0.107 GeV, respectively, from the Particle Data Group [14]. The fitted mass is close to the accepted value but the width is wider and this is expected from the effects of fitting a peak that is close to the width of the bins.

A fit of coupling the intensity and phase of the 2^{+1} into a χ^2 fit resulted in a narrower width but fails to describe the phase shift past 1.45 GeV. The phase shift is fit for a constant phase minus the phase of the 2^{+1} . The fit is shown in Fig. 4 and resulted in a mass and width of 1.32 ± 0.01 and 0.14 ± 0.01 GeV.

By including the 1^{-1} and 2^{+1} interference, illustrated in Fig. 5, is the a_2 is found with a mass of 1.343 ± 0.003 and a width of 0.174 ± 0.003 GeV. With the E852 mass and width values for the $\pi_1(1400)$ of 1.37 and 0.385 GeV, the π_1 amplitude was fit to have a mass and width of 1.39 ± 0.23 and 0.58 ± 0.05 GeV. The results initially look promising but the result of the fit of the phase is poor. In the resonance spectra the acceptance decreasing from 0.8 to 0.15 % in the last five bins in the fit, the shift in phase difference is possibly a product of poorly known fits due to a combination of low statistics in the data (9 to 38 events per bin) and rapidly changing acceptance.

6. Conclusion

The inspiration of this analysis was to look for an exotic state using photoproduction in a reaction restricted to charge exchange. In previous searches, the presence of an exotic was conclusive for neutral exchanges but not consistent for charge exchanges within the same experiments [15].

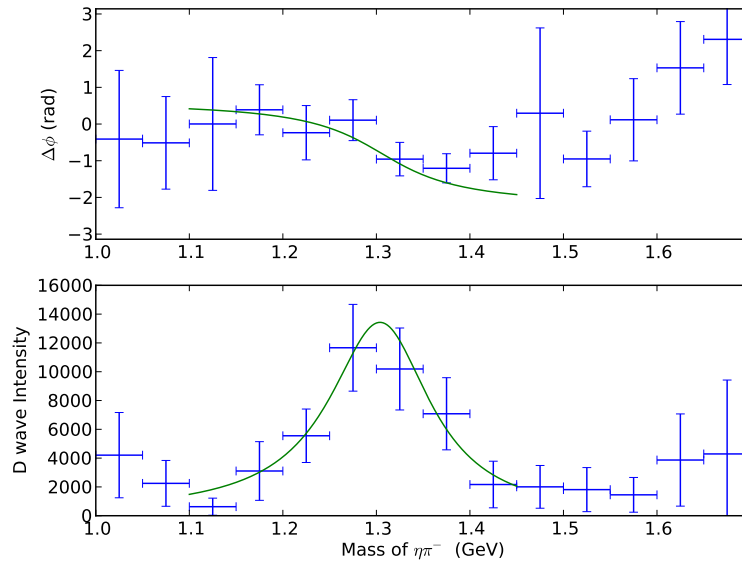


Figure 4: Fit 2: Coupled phase motion (top) and intensity (bottom) of the mass dependent fit for a_2 . Fitting the BW intensity function, the mass and width if the a_2 is 1.32 ± 0.01 and 0.14 ± 0.01 GeV.

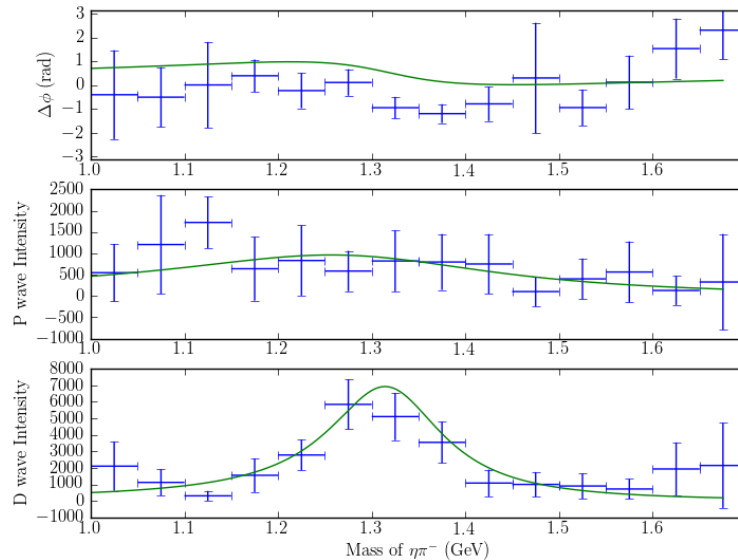


Figure 5: Fit 3: Coupled phase motion (top), intensity of P wave (middle), and intensity of D wave (bottom) of the mass dependent fit for a_2 and π_1 , for positive reflectivity. The mass and width of the fitted a_2 is 1.343 ± 0.003 and 0.174 ± 0.003 GeV. The mass and width of π_1 is 1.39 ± 0.23 and 0.58 ± 0.05 GeV but the phase difference of the fit does not model the data.

This has led to the counter arguments of the exotic interference is due to background or model dependencies. The use of photoproduction is the next step in exploring the possibility of exotics. The PWA of the $\eta\pi^-$ mass spectrum in photoproduction showed a peak in the $J^P = 2^+$ partial wave spectrum but did not show a strong 1^- contribution from the exotic candidate. The fit of the partial wave spectrum resulted in a mass and width of the $J^P = 2^+$ to be consistent with the $a_2(1320)$. However, further analysis of the phase difference between the $J^P = 2^+$ and $J^P = 1^-$ along with the intensities resulted in no evidence of the $\pi_1(1400)$ exotic. This analysis is sensitive to the π_1 if it is produced at the hypothesized strength of 30 to 50 % of the a_2 . The lack of evidence of an exotic at the proposed intensities adds to the excitement of the next generation of results to come from CLAS12 and GlueX at Jefferson Lab, COMPASS at CERN, and Panda at GSI.

References

- [1] S. U. Chung, Evidence for Exotic $J^{pc} = 1^{-+}$ Meson Production in the Reaction $\pi^- p \rightarrow \eta\pi^- p$ at 18 GeV/c, Phys. Rev. D, 60, (1999).
- [2] A. P. Szczepaniak, Role of Photo Production in Exotic Meson Searches, Phys. Lett. B, 516, (2001), 72-76.
- [3] P. Eugenio, Search for New Forms of Hadronic Matter in Photoproduction, JLAB-E04-005, (2003).
- [4] D. S. Carman, GlueX: The Search for Gluonic Excitations at Jefferson Laboratory, Hadron Spectroscopy: Eleventh International Conference, (2006).
- [5] S. U. Chung, Formulas for Partial-Wave Analysis Version II, BNL-QGS-93-05, (1993).
- [6] D. J. Herndon, Generalized Isobar Model Formalism, Phys. Rev. D, 11, 11, (1975).
- [7] J. H. Jee, The BNL Four-Body Partial Wave Analysis System, based on BNL-QGS-93-05.
- [8] G. S. Adams, Exotic Meson Spectroscopy from BNL E852, Hadron Spectroscopy: Eleventh International Conference, (2006).
- [9] J. J. Manak, Partial-Wave Analysis of the $\eta\pi^+\pi^-$ System Produced in the Reaction $\pi^- p \rightarrow \eta\pi^+\pi^- n$ at 18 GeV/c, arXiv:hep-ex/0001051v1 21Jan2000.
- [10] M. Nozar, Search for the Photo-Excitation of Exotic Mesons in the $\pi^+\pi^+\pi^-$ System, CLAS-ANALYSIS, 2006-102, (2006).
- [11] J. Cummings, An Object-Oriented Approach to Partial Wave Analysis, arXiv:physics/0309052v1.
- [12] S. Chung, Spin Formalisms, BNL, 76975-2006-IR.
- [13] S. Chung, Positivity Conditions on the Spin Density Matrix: A Simple Parameterization, Phys. Rev. D, 11, 633, (1975).
- [14] H. Bichsel, Passage of Particles Through Matter, Journal of Physics G: Nuclear and Particle Physics, 33, (2006), 268-269.
- [15] C. Amsler, Mesons Beyond the Naive Quark Model, Physics Reports, 387(2004), 61-117.